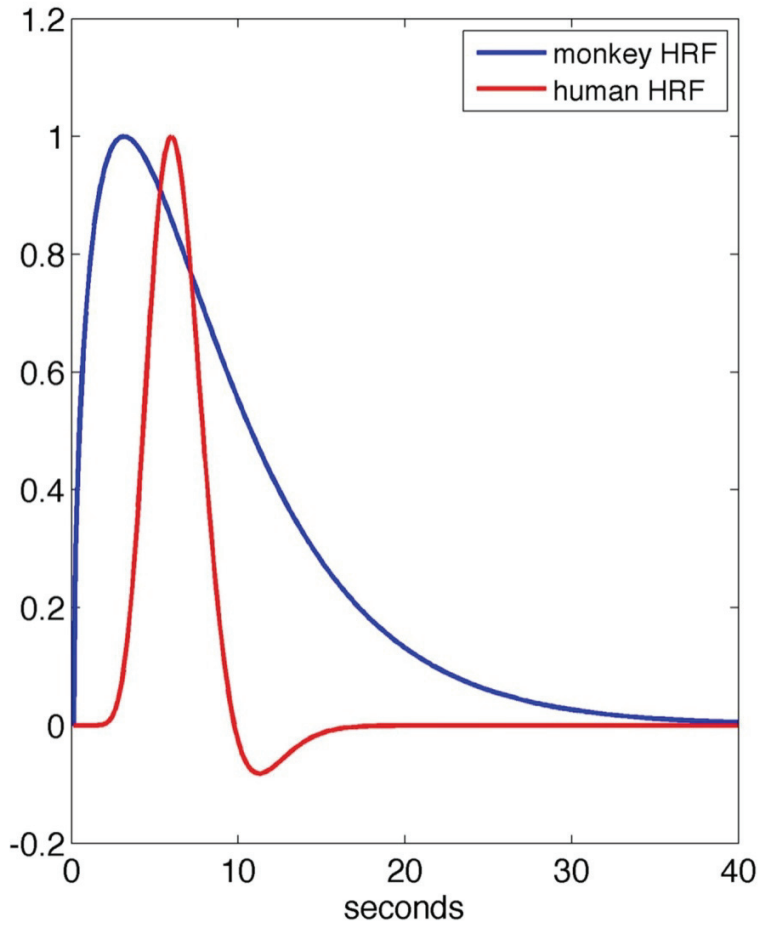
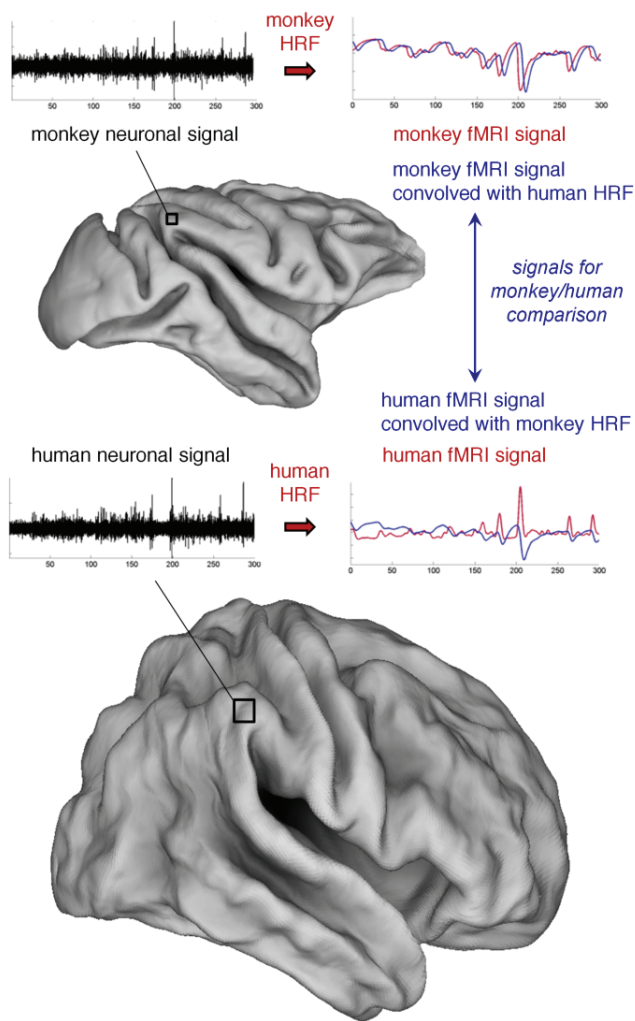


**Supplementary Figure 1. Monkey and human hemodynamic response functions.**



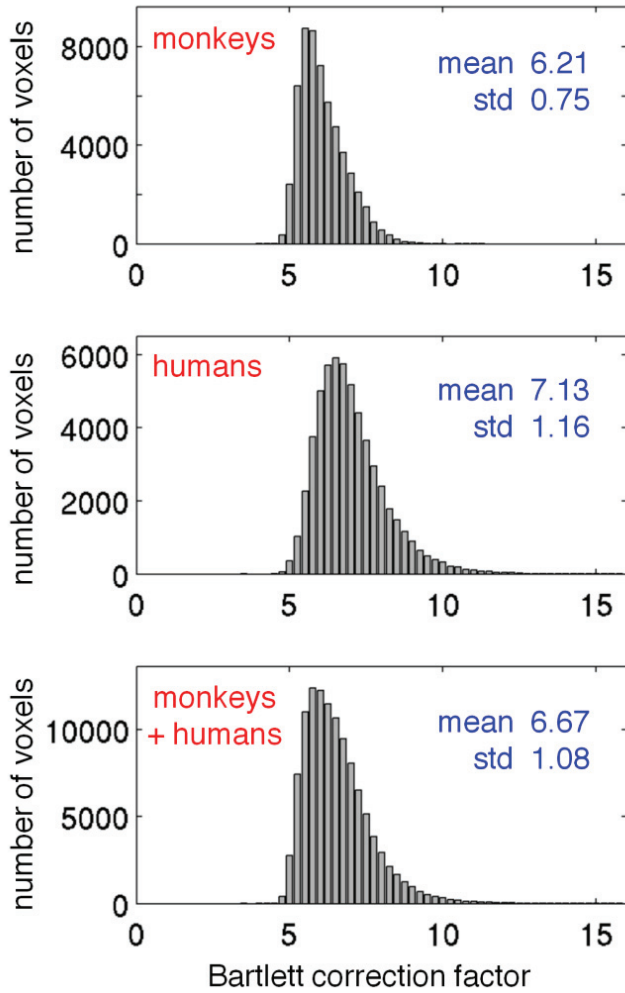
The plot shows the monkey and human hemodynamic response functions (HRFs) used in our study. The human HRF is the canonical HRF implemented in SPM5.0 for classical activation analysis of human fMRI data, whereas the monkey HRF is the one currently in use in our monkey fMRI laboratory<sup>26,29</sup>. The monkey HRF, which is originally negative due to the MION-CBV measure, has been inverted to simplify comparison with the human HRF.

**Supplementary Figure 2. Temporal alignment of monkey and human fMRI signals.**



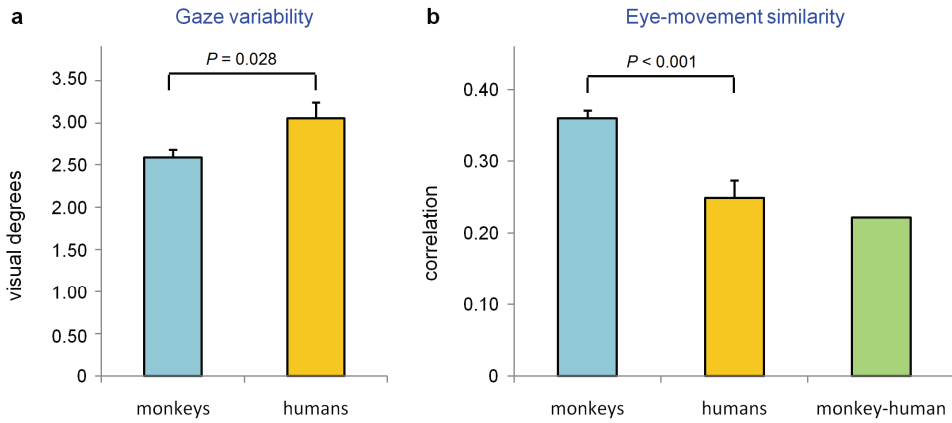
Due to differences in the hemodynamic response functions (HRF), the direct comparison between fMRI signals of monkeys and humans may typically show low correlation, even when the neuronal activity is highly correlated. In this regard, the HRF in monkey and human data can be tentatively equalized by convolving the monkey and human data with the human and monkey HRF, respectively. The cross-species HRF convolution increases the sensitivity for the detection of brain areas for which neuronal activity is correlated in the two species.

**Supplementary Figure 3. Value distribution of the Bartlett correction factor for signal autocorrelation.**



The Bartlett correction factor for signal autocorrelation was computed for the gray-matter voxels of the average monkey (deformed to human) and human datasets. The histograms of the values in the monkey and the brain are shown, separately and jointly, along with the results of descriptive statistics (including mean and standard deviation) calculated for them.

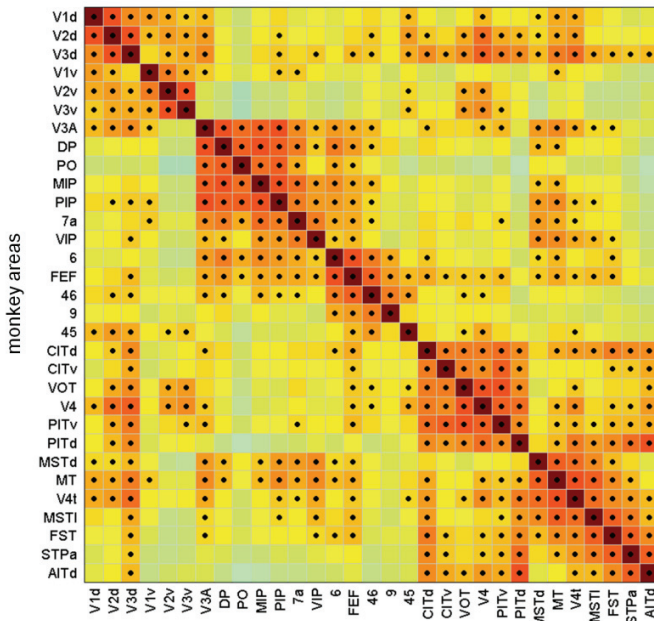
**Supplementary Figure 4. Analysis of monkey and human eye gaze during natural vision.**



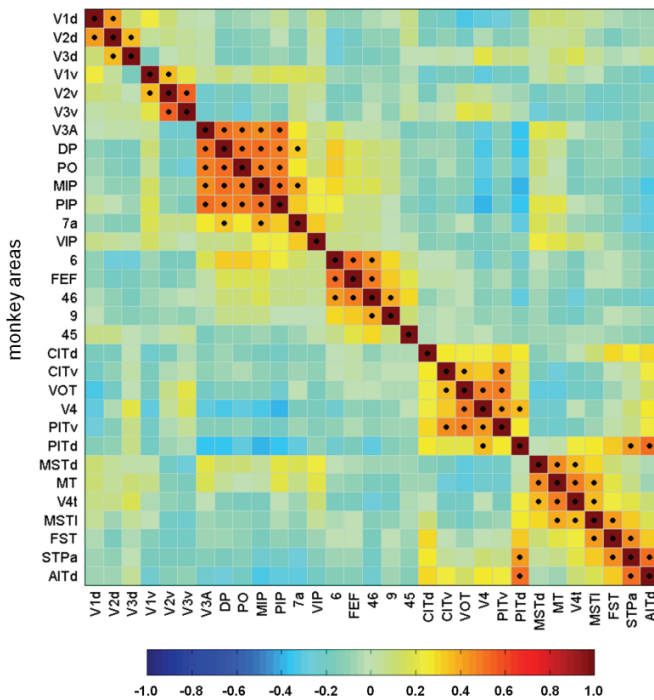
**(a)** Variability in the eye-traces during natural vision across monkeys ( $n = 4$ ) and humans ( $n = 24$ ). **(b)** Temporal correlations of eye-movement signals across monkeys, across humans, and between monkeys and humans. Error bars show s.e.m. Probabilities related to significant differences between groups, as assessed by means of a two-tailed unpaired t-test, are reported in the plots.

**Supplementary Figure 5. Activity correlation between monkey areas before and after common signal regression.**

**a Intra-species activity correlation before common signal regression**



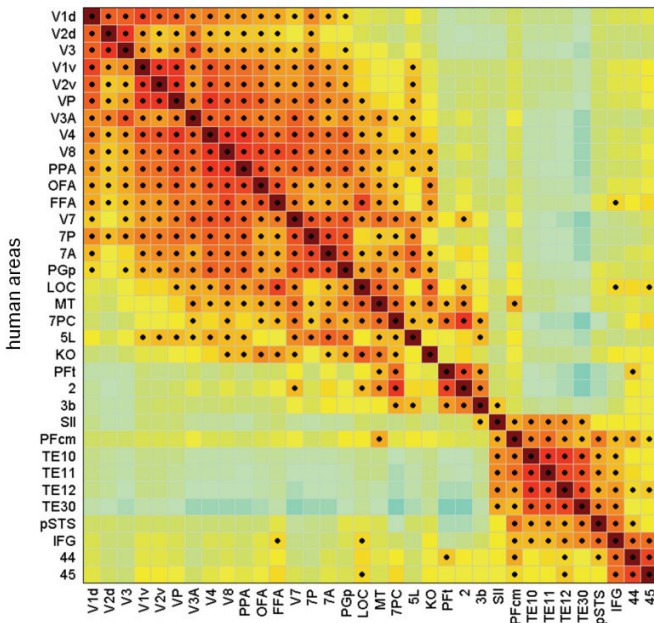
**b Intra-species activity correlation after common signal regression**



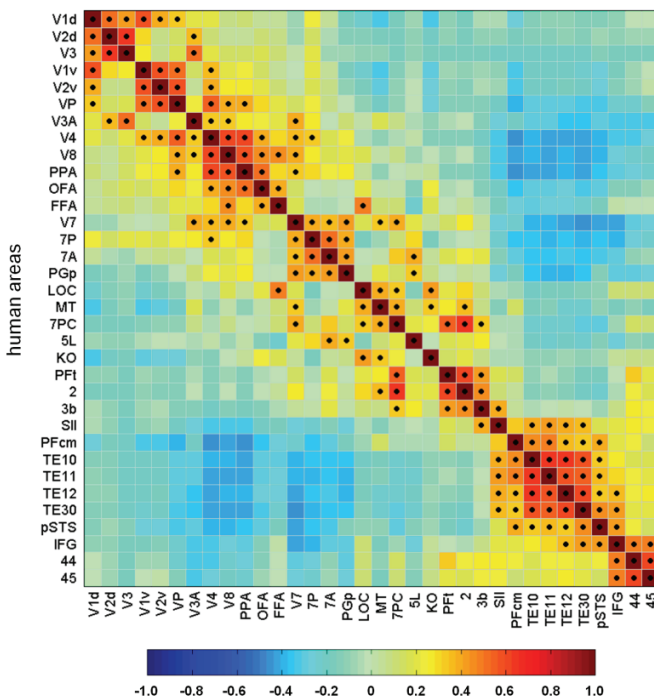
Intra-species activity correlations between selected areas in the monkey (a) before and (b) after common signal regression. Monkey areas are sorted so that those with larger mutual correlations are close to each other. Significant Pearson's correlations (FDR of  $q < 0.001$ ) are marked with a black dot.

**Supplementary Figure 6. Activity correlation between human areas before and after common signal regression.**

**a Intra-species activity correlation before common signal regression**



**b Intra-species activity correlation after common signal regression**



Intra-species activity correlations between selected areas in the human (a) before and (b) after common signal regression. Human areas are sorted so that those with larger mutual correlations are close to each other. Significant Pearson's correlations (FDR of  $q < 0.001$ ) are marked with a black dot.

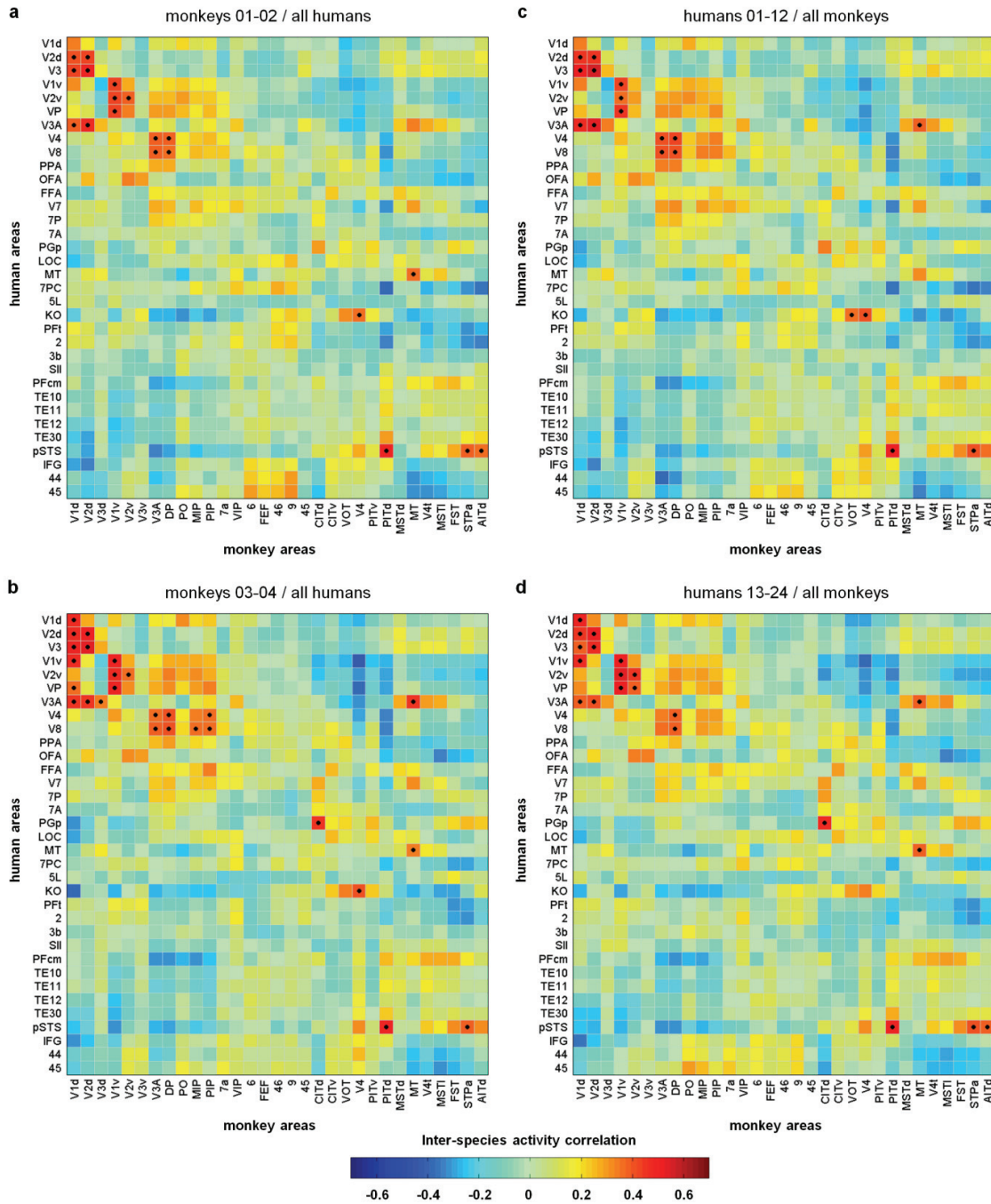








**Supplementary Figure 9. Reliability of inter-species activity correlation matrices.**



We assessed the reliability of the inter-species activity correlations, by splitting the monkey and human datasets in halves (monkeys 01-02 and 03-04, humans 01-12 and 13-24). We calculated a correlation matrix between monkey and human functional responses for: **(a)** monkeys 01-02 and all humans; **(b)** monkeys 03-04 and all humans; **(c)** humans 01-12 and all monkeys; **(d)** humans 13-24 and all monkeys. Significant functional correspondences, defined on the basis of the Pearson's correlation test (FDR of  $q < 0.001$ ), are marked with a black dot.

**Supplementary Table 1. Inter-species activity correlation between anatomically-corresponding visual areas.**

	V1d	V1v	V2d	V2v
Before common signal regression	$r = 0.64$ $P < 0.001$	$r = 0.66$ $P < 0.001$	$r = 0.67$ $P < 0.001$	$r = 0.58$ $P < 0.001$
After common signal regression	$r = 0.42$ $P < 0.001$	$r = 0.48$ $P < 0.001$	$r = 0.49$ $P < 0.001$	$r = 0.37$ $P < 0.001$
After common signal regression (1 <sup>st</sup> movie repetition for the monkeys)	$r = 0.34$ $P < 0.001$	$r = 0.36$ $P < 0.001$	$r = 0.47$ $P < 0.001$	$r = 0.42$ $P < 0.001$
After common signal regression (2 <sup>nd</sup> movie repetition for the monkeys)	$r = 0.40$ $P < 0.001$	$r = 0.47$ $P < 0.001$	$r = 0.38$ $P < 0.001$	$r = 0.38$ $P < 0.001$
After common signal regression (3 <sup>rd</sup> movie repetition for the monkeys)	$r = 0.34$ $P < 0.001$	$r = 0.42$ $P < 0.001$	$r = 0.39$ $P < 0.001$	$r = 0.34$ $P < 0.001$
After common signal regression (4 <sup>th</sup> movie repetition for the monkeys)	$r = 0.39$ $P < 0.001$	$r = 0.40$ $P < 0.001$	$r = 0.48$ $P < 0.001$	$r = 0.38$ $P < 0.001$
After common signal regression (5 <sup>th</sup> movie repetition for the monkeys)	$r = 0.50$ $P < 0.001$	$r = 0.51$ $P < 0.001$	$r = 0.49$ $P < 0.001$	$r = 0.43$ $P < 0.001$
After common signal regression (6 <sup>th</sup> movie repetition for the monkeys)	$r = 0.51$ $P < 0.001$	$r = 0.47$ $P < 0.001$	$r = 0.50$ $P < 0.001$	$r = 0.30$ $P = 0.001$

The correlations between monkey and human V1d, V1v, V2d and V2v were measured on the whole datasets before and after the regression of the common component, respectively; in this second case, we also used subsets of the monkey data referring to each movie repetition. For each correlation in the table, the associated probability is also given.

**Supplementary Note. Theoretical considerations on monkey and human hemodynamic response functions.**

In the present section we provide theoretical considerations regarding the possibility of detecting temporal similarities between brain activity in monkeys and in humans, based on fMRI measurements. Let us denote with  $n_M(t)$  and  $n_H(t)$  two time-courses related to neuronal activity in the monkey and human brain respectively. Their frequency-domain representations are indicated with  $N_M(f)$  and  $N_H(f)$ . If the two time-series are identical, we would have  $n_M(t) = n_H(t)$  and  $N_M(f) = N_H(f)$ . Since the fMRI signal is assumed to be related to neuronal activity through the convolution with an hemodynamic response function (HRF), we can model such a relationship as:

$$\begin{aligned} f_M(t) &= n_M(t) \otimes k_M(t) \\ f_H(t) &= n_H(t) \otimes k_H(t) \end{aligned} \quad (1)$$

where  $f_M(t)$  and  $f_H(t)$  represent the monkey and human fMRI signals, respectively, and  $k_M(t)$  and  $k_H(t)$  represent the monkey and human HRFs. In the frequency domain, the spectrum of the fMRI signals results from the product of the spectrum of the neuronal activity  $N(f)$  (typically broad-band) and the spectrum of the HRF  $K(f)$  (with low-pass properties). By applying a Fourier transformation to eq. (1), we obtain:

$$\begin{aligned} F_M(f) &= N_M(f) \cdot K_M(f) \\ F_H(f) &= N_H(f) \cdot K_H(f) \end{aligned} \quad (2)$$

In the hypothetical case for which the neuronal activity in monkeys and humans is identical, it is clear that a mismatch between the recorded fMRI signals in the two species could potentially be due to a difference between HRFs. In particular, it is well-known that the MION-enhanced monkey fMRI is characterized by an HRF that is slower with respect to the typical human HRF, and has reversed polarity (for further details, see Fig. S1).

In order to allow for the different HRFs in the two species, we convolved the monkey and human fMRI signals with the human and monkey HRF, respectively. The convolved fMRI time-courses in monkeys and humans, indicated with  $s_M(t)$  and  $s_H(t)$  respectively, are:

$$\begin{aligned} s_M(t) &= f_M(t) \otimes k_H(t) = [n_M(t) \otimes k_M(t)] \otimes k_H(t) \\ s_H(t) &= f_H(t) \otimes k_M(t) = [n_H(t) \otimes k_H(t)] \otimes k_M(t) \end{aligned} \quad (3)$$

Taking into account that the convolution is commutative, we can write:

$$\begin{aligned} s_M(t) &= n_M(t) \otimes [k_M(t) \otimes k_H(t)] = n_M(t) \otimes k_T(t) \\ s_H(t) &= n_H(t) \otimes [k_H(t) \otimes k_M(t)] = n_H(t) \otimes k_T(t) \end{aligned} \quad (4)$$

where  $k_T(t)$  represents the convolution between the HRFs in the two species. It can be observed from eq. (4) that, if  $n_M(t) = n_H(t)$ , we would have also  $s_M(t) = s_H(t)$ . If the two neuronal signals are not identical, the analysis of the temporal correlation between  $s_M(t)$  and  $s_H(t)$  can provide valuable information about similarities between  $n_M(t)$  and  $n_H(t)$ . However, it should be taken into account that the convolution of the neuronal signals with  $k_T(t)$  limits the frequency band for which potential differences can be assessed, due to the typical HRF low-pass properties. This is not necessarily a limitation of the convolution procedure, as the fMRI signals are already filtered by the HRF. Conversely, by convolving the monkey and human fMRI signals with the human and monkey HRFs, respectively, the spectral content is equalized. In fact, by writing eq. (4) in the frequency domain, it turns out that:

$$\begin{aligned} S_M(f) &= N_M(f) \cdot K_T(f) \\ S_H(f) &= N_H(f) \cdot K_T(f) \end{aligned} \tag{5}$$

It is worth noting that low-frequency components in  $n_M(t)$  and  $n_H(t)$  may predominate, resulting in a large temporal autocorrelation. By using the temporal correlation as similarity metric, it is likely that the measured correspondence between  $s_M(t)$  and  $s_H(t)$ , will be larger than that between  $n_M(t)$  and  $n_H(t)$ . Based on these considerations, we conclude that, in measuring the correlation between  $s_M(t)$  and  $s_H(t)$ , it is important to apply statistical methods to account for the autocorrelation in the time-series.